

## Isomeric cross-section ratio for the formation of $^{73m,g}\text{Se}$ in various nuclear processes

S. M. Qaim and A. Mushtaq\*

*Institut für Chemie I (Nuklearchemie), Kernforschungsanlage Jülich GmbH, D-5170 Jülich, Federal Republic of Germany*

M. Uhl

*Institut für Radiumforschung und Kernphysik, Universität Wien, Wien, Austria*

(Received 21 March 1988)

The isomeric cross-section ratio  $\sigma_m/(\sigma_m + \sigma_g)$  for the formation of  $^{73m,g}\text{Se}$  was determined in the  $^{70}\text{Ge}(\alpha, n)$  reaction over the energy range of 13–27 MeV, in the  $^{\text{nat}}\text{Ge}({}^3\text{He}, xn)$  process over 13–24 MeV, in the  $^{75}\text{As}(p, 3n)$  reaction over 25–45 MeV, and in the  $^{75}\text{As}(d, 4n)$  reaction over 28–56 MeV. Measurements were done radiochemically using the “stacked-foil” technique. In  $(\alpha, n)$  and  $({}^3\text{He}, xn)$  processes the ratio is relatively high at low incident particle energies but decreases with increasing energy. In  $(p, 3n)$  and  $(d, 4n)$  reactions, on the other hand, it is practically constant. Statistical model calculations taking into account precompound emission were carried out on the four processes investigated in this work as well as on the  $^{74}\text{Se}(n, 2n)$  reaction reported in the literature. The total cross section  $(\sigma_m + \sigma_g)$  is described well by the calculation. The calculated isomeric cross-section ratio depends strongly on the input level scheme of the product nucleus. In general, however, the statistical model, under a suitable set of global assumptions, can reproduce the isomeric cross-section ratio in all the five nuclear processes.

### I. INTRODUCTION

The isomeric cross-section ratio for a pair of isomeric states is known to depend strongly on the spins of the isomers concerned, as well as on the spins of the higher lying levels populating the isomers. Experimental and theoretical studies on the isomeric cross-section ratios, especially as a function of incident particle energy, should therefore lead to useful information on the spin-cutoff parameter as well as on the level structure of the product nucleus.

We chose to investigate the isomeric pair  $^{73m,g}\text{Se}$ . A simplified decay scheme (cf. Refs. 1 and 2) is given in Fig. 1. The separation energy between the two isomeric levels is only 25.7 keV but the spins differ considerably. Both the states can be populated via five nuclear processes, viz.  $^{70}\text{Ge}(\alpha, n)$ ,  $^{\text{nat}}\text{Ge}({}^3\text{He}, xn)$ ,  $^{75}\text{As}(p, 3n)$ ,  $^{75}\text{As}(d, 4n)$ , and  $^{74}\text{Se}(n, 2n)$ . The  $(n, 2n)$  and  $(d, 4n)$  processes were investigated previously (cf. Refs. 3–6). In the case of other reactions, however, measurements were reported only for the 7.1 h  $^{73g}\text{Se}$  (Refs. 7–9). We investigated the first four processes experimentally over wide energy ranges of incident particles and performed model calculations for all the five reactions.

### II. EXPERIMENTAL

Cross sections were measured as a function of incident particle energy using the “stacked-foil” technique (cf. Refs. 10–12). For studies of  $\alpha$ - and  ${}^3\text{He}$ -particle induced reactions on germanium, thin samples were prepared by electrolytic deposition of Ge on Cu backing (cf. Ref. 13). Several stacks consisting of electroplated foils and various absorber and beam current monitor foils were irradiated for 20 min at 40 nA with 28 MeV  $\alpha$  particles or 36

MeV  ${}^3\text{He}$  particles at the compact cyclotron (CV 28). Beam currents were measured as described earlier.<sup>12</sup> In both  ${}^3\text{He}$ - and  $\alpha$ -particle induced reactions measurement of the 7.1 h  $^{73g}\text{Se}$  activity via  $\gamma$ -ray spectrometry was relatively straightforward and was done using the 361 keV  $\gamma$  line ( $I_\gamma = 97\%$ ). The excitation function of the  $^{70}\text{Ge}(\alpha, n)^{73g}\text{Se}$  reaction could be determined in absolute terms since in the investigated energy range no other reaction contributes. In the case of  ${}^3\text{He}$ -induced process, however, only the effective cross section could be obtained due to the contribution of several reactions like  $^{72}\text{Ge}({}^3\text{He}, 2n)^{73g}\text{Se}$ ,  $^{73}\text{Ge}({}^3\text{He}, 3n)^{73g}\text{Se}$ , and  $^{74}\text{Ge}({}^3\text{He}, 4n)^{73g}\text{Se}$ .

Measurement of  $^{73m}\text{Se}$  ( $T_{1/2} = 40$  min) in  ${}^3\text{He}$ - and  $\alpha$ -particle induced reactions on Ge presented difficulty due to the strong copper matrix activity. After irradiation each electroplated foil was therefore treated with 3 ml of warm 3%  $\text{H}_2\text{O}_2$ . The very thin layer of Ge and the radioselenium went in solution and thus got separated from the Cu backing. The solution was then subjected to  $\gamma$ -ray spectrometry and the activities of  $^{73m}\text{Se}$  and  $^{73g}\text{Se}$  were determined. A correction for the radiochemical yield was not necessary since only relative measurements were done. The activity of  $^{73m}\text{Se}$  was determined via the 254 keV  $\gamma$ -ray. Since this  $\gamma$ -ray has an abundance of only 2.5% (Ref. 1) the results were checked by an independent method involving an analysis of the growth and decay curve of  $^{73g}\text{Se}$ . The two results were found to be in agreement. From the experimental data the isomeric cross-section ratio  $\sigma_m/(\sigma_m + \sigma_g)$  was determined taking into account the branching ratio of  $^{73m}\text{Se}$ .

For studies of proton- and deuteron-induced reactions on arsenic, thin target samples were prepared by electrolytic deposition of As on Cu or Al backing (cf. Ref. 14). Similar to studies described above, several stacks were ir-

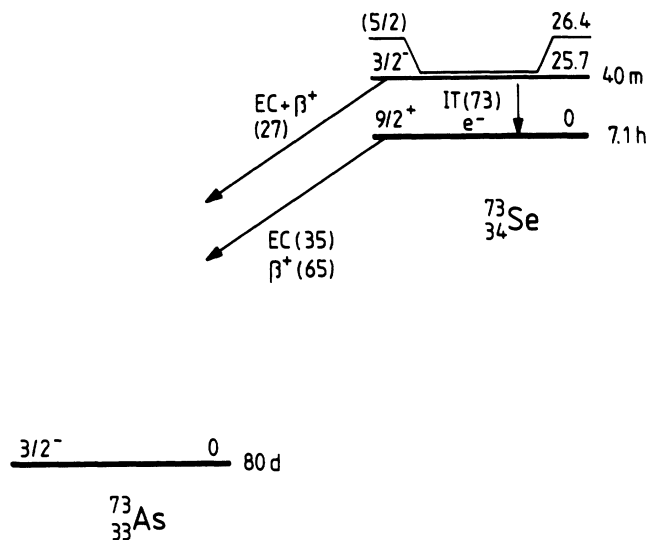


FIG. 1. Simplified decay scheme of isomeric pair  $^{73m,g}\text{Se}$ .

radiated for 20 min at 50 nA with 45 MeV protons or 56 MeV deuterons at the isochronous cyclotron (JULIC). The details on the measurement of the 7.1 h  $^{73g}\text{Se}$  have already been described.<sup>15</sup> In the case of  $^{73m}\text{Se}$  electroplating was done invariably on Al backing to suppress the matrix activity. Measurement could then be done without chemical separation.

The total errors in the absolute cross sections for the formation of the ground state were about 16% as described in detail earlier.<sup>15</sup> The errors in the isomeric cross-section ratios ranged between 10 and 20%. The energy degradation calculation in the stacked foils also contained some error. It was about  $\pm 0.5$  MeV up to a projectile energy of 15 MeV, and about  $\pm 0.3$  MeV at higher energies.

### III. NUCLEAR MODEL CALCULATIONS

Nuclear reaction cross sections were calculated using the statistical model taking into account the preequilibrium effects for the first chance emission of each particle. Direct interactions were not considered. For the nucleon-induced reactions a consideration of direct reactions would reduce the cross sections by 5–10%. For the composite projectiles, in particular for the loosely bound deuteron and for  $^3\text{He}$ , the effect of direct interactions might be more complicated due to breakup fusion contributions.

For calculation of transmission coefficients of various particles, the following global set of optical model parameters were used:

$n$ , Rapaport *et al.*<sup>16</sup> This potential is based on data for energies between 7 and 30 MeV. For energies  $< 7$  MeV it was slightly modified;

$p$ , Mani *et al.*;<sup>17</sup>

$d$ , Hinterberger *et al.*;<sup>18</sup>

$^3\text{He}$ , Becchetti and Greenlees;<sup>19</sup>

$\alpha$ , McFadden and Satchler.<sup>20</sup>

The transmission coefficients for photons were expressed through the  $\gamma$ -ray strength functions  $f_{XL}(\epsilon_\gamma)$  for multipole radiation of type  $XL$ . For  $E1$  radiation the Brink-Axel model<sup>21</sup> with global parameters was used and for  $M1$ ,  $E2$ ,  $M2$ ,  $E3$ , and  $M3$  radiations the Weisskopf model was used.<sup>22</sup> In the latter case the strength amounted to 1.4 Weisskopf units (WU) for  $M1$  and 1 WU for  $E2$ – $M3$ . With the help of an  $XL$ -independent factor the sizes of  $f_{XL}(\epsilon_\gamma)$  were so normalized that the available experimental  $s$ -wave radiation widths were reproduced.

In the calculations of emissions from equilibrated compound nucleus the conservation of angular momentum and parity was taken into account. For low excitation energies of the product nucleus the known nuclear levels (cf. Refs. 1 and 2) were used. In the continuum region, however, a level density formula derived from a combination of “constant temperature” form and the model of Kataria *et al.*<sup>23</sup> was applied. Its parameters were deduced from the number of low-lying levels and the density of neutron resonances.<sup>24</sup> The spin distribution of the level density was characterized by the effective moment of inertia  $\Theta_{\text{eff}}$ , or better by its ratio to rigid body moment of inertia  $\Theta_{\text{rig}}(\eta = \Theta_{\text{eff}}/\Theta_{\text{rig}})$ . Since isomeric cross-section ratios are expected to depend strongly on the effective moment of inertia, all the calculations were performed for  $\eta = 1.0$  and  $\eta = 0.5$ .

The preequilibrium emission of particles was treated in the framework of the exciton model having the following ingredients. The particle emission rates were determined via the method of Gadioli *et al.*<sup>25</sup> when nucleons were used as projectiles, and via that of Kalbach<sup>28</sup> in case of composite particles as projectiles. The rates of particle-hole pair formation were calculated by the method of Oblozinsky *et al.*<sup>27</sup> including an expression suggested by Kalbach<sup>28</sup> for the average matrix element of the residual interactions. A conventional pairing shift was applied to all particle-hole state densities. The projectile-dependent initial particle and hole numbers ( $p_0, h_0$ ) used were (2,1) for nucleons, (3,1) for deuterons, (4,1) for  $^3\text{He}$  particles, and (4,0) for  $\alpha$  particles. Because of their importance, for isomer ratios the angular momentum effects in preequilibrium emission were also considered approximately. The distribution of the emission spectrum  $d\sigma_{\alpha\beta}/d\epsilon_\beta$  (itself calculated using an angular momentum independent model) among the individual spins of the residual nucleus was performed taking into account the conservation of angular momentum and assuming spin-dependent level densities for a given number of particles and holes with spin-distribution parameters which depend<sup>29</sup> on the number of excitons and not on the excitation energy.

The choice of discrete nuclear levels of  $^{73}\text{Se}$  was rather critical. According to the latest information<sup>2</sup> the level scheme of  $^{73}\text{Se}$  contains two rotational bands: one with levels of positive parity, which in  $\gamma$ -decay primarily populate the  $\frac{9}{2}^+$  ground state, and the other with levels of negative parity, whose  $\gamma$ -decays lead to the formation of the  $\frac{3}{2}^-$  isomer. We adopted the level scheme given in Ref. 2 up to 998.99 keV. For levels where spins and parities are not established, the values suggested by Zell *et al.*<sup>30</sup> or from systematic considerations were used. The  $\gamma$ -branching ratios for all those levels were taken

from Ref. 2. Between 1.0 and 1.58 MeV (continuum edge) the number of levels given by the level density formula were used. Their spins and parities were chosen from a random distribution given by the formula. In addition to these generated levels two known levels (at 1179.9 keV,  $\frac{11}{2}^-$  and 1553.14 keV,  $\frac{13}{2}^-$ ) belonging to the rotational band with negative parity were also introduced. Thus the level scheme of  $^{73}\text{Se}$  used in calculations consisted of 44 discrete levels. This is denoted as LS1 in all the calculational results. Calculations were also done using a slight variation in the level scheme. The third level (at 26.4 keV,  $\frac{5}{2}$ ) suggested by Zell *et al.*<sup>30</sup> and shown in Fig. 1 was neglected and it was assumed that the  $\gamma$  transitions to this level populate the isomeric state. The results obtained using this level scheme (43 levels) are denoted as LS2.

All the calculations were performed using the code MAURINA (Ref. 31) which can treat sequential emission of up to six different particles and incorporates up to 50 discrete levels for each product nucleus.

#### IV. RESULTS AND DISCUSSION

##### Total cross sections

In order to demonstrate the reliability of the present model calculations, at first total cross sections were considered. The excitation functions of the  $^{70}\text{Ge}(\alpha, n)^{73}\text{Se}$ ,  $^{75}\text{As}(p, 3n)^{73}\text{Se}$ ,  $^{75}\text{As}(d, 4n)^{73}\text{Se}$ , and  $^{74}\text{Se}(n, 2n)^{73}\text{Se}$  reactions are reproduced in Figs. 2–5. The experimental results for the  $^{74}\text{Se}(n, 2n)$  process have been taken from the literature.<sup>4,5</sup> The data for the  $^{75}\text{As}(p, 3n)$  and  $^{75}\text{As}(d, 4n)$  reactions are based on our recent experimental results,<sup>15</sup> adjusted for the branching ratio of  $^{73m}\text{Se}$ . For the  $^{75}\text{As}(d, 4n)$  reaction some available literature values<sup>6</sup> are also given. The  $^{70}\text{Ge}(\alpha, n)$  reaction cross sections were

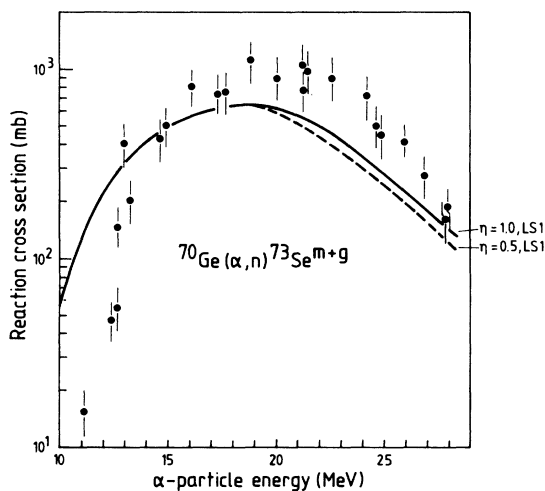


FIG. 2. Excitation function of  $^{70}\text{Ge}(\alpha, n)^{73m, g}\text{Se}$  reaction. Solid points describe the experimental data and curves give the results of model calculations using nuclear level scheme 1 (LS1: 44 discrete levels) and  $\eta$  values of 1.0 and 0.5 (for details see text).

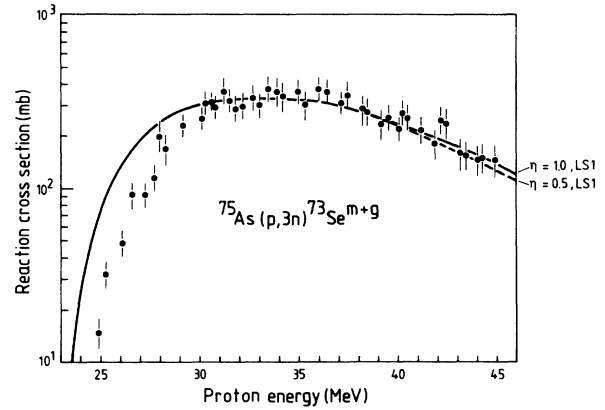


FIG. 3. Excitation function of  $^{75}\text{As}(p, 3n)^{73m+g}\text{Se}$  reaction. Other details are the same as for Fig. 2.

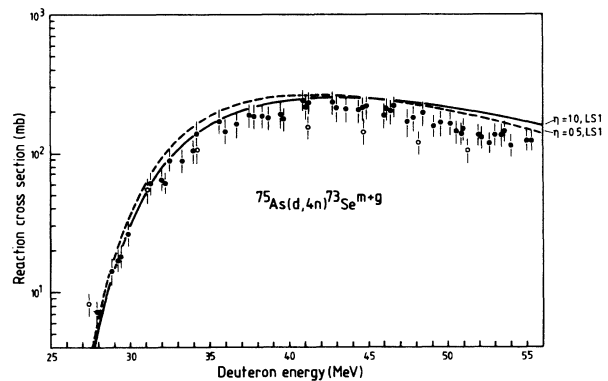


FIG. 4. Excitation function of  $^{75}\text{As}(d, 4n)^{73m+g}\text{Se}$  process. Solid points describe our experimental data and open points those of Ref. 6. Other details are the same as for Fig. 2.

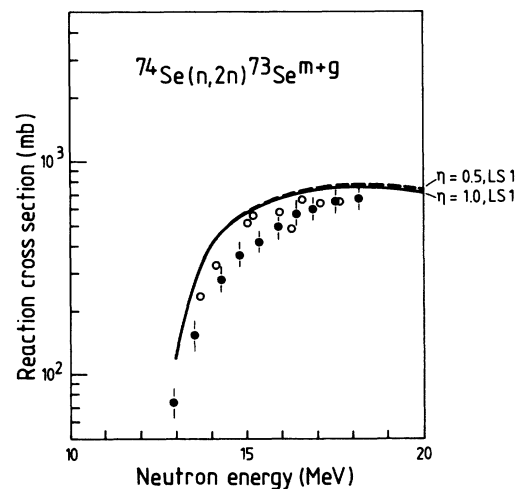


FIG. 5. Excitation function of  $^{74}\text{Se}(n, 2n)^{73m+g}\text{Se}$  process. Experimental data (solid and open points) are from Refs. 4 and 5. Other details are the same as for Fig. 2.

measured in this work. In the interactions of  $^3\text{He}$  particles with  $^{\text{nat}}\text{Ge}$ , due to difficulty in resolution of various contributing processes, absolute cross sections could not be determined.

The results of model calculations are also given in Figs. 2–5. The experimental and theoretical results for the  $^{70}\text{Ge}(\alpha, n)$  reaction (Fig. 2) are somewhat discrepant. There appears to be an energy shift of about 2 MeV and the cross sections at the maxima also differ. Experimentally, the excitation function was obtained using eight different stacks covering several overlapping energy regions. Theoretically,  $\alpha$ -transmission coefficients were calculated using the optical model parameters described above as well as the Huizenga and Igo parameters.<sup>32</sup> The results were also similar. A calculation using the code ALICE (Ref. 33) also gave similar results. The discrepancy appears to be genuine but is presently not explainable.

For the  $^{75}\text{As}(p, 3n)$  process (Fig. 3) the calculation slightly overestimates the initial increasing part of the excitation curve; the maximum and the tail, however, are reproduced well. For the  $^{75}\text{As}(d, 4n)$  reaction (Fig. 4) the experimental and theoretical results are in good agreement. A comparison of the experimental and theoretical data for the  $^{74}\text{Se}(n, 2n)$  process (Fig. 5) also shows fairly good agreement.

In Figs. 2–5 the results of model calculations obtained using only one nuclear level scheme of the product nucleus (LS1) are shown. Similar results were obtained using LS2. Furthermore, for each of the four processes considered the total cross section was found to be practically the same whether  $\eta=1.0$  or 0.5 was used. The level scheme and the effective moment of inertia have therefore no drastic effect on the total cross section of a process which appears to be reproduced with good reliability by the model calculations described here.

#### Isomeric cross-section ratios

The experimental results on the isomeric cross-section ratio  $\sigma_m/(\sigma_m+\sigma_g)$  for the isomeric pair  $^{73m,g}\text{Se}$  produced via five nuclear processes, viz.  $^{70}\text{Ge}(\alpha, n)$ ,  $^{\text{nat}}\text{Ge}(^3\text{He}, xn)$ ,  $^{75}\text{As}(p, 3n)$ ,  $^{75}\text{As}(d, 4n)$ , and  $^{74}\text{Se}(n, 2n)$ , are given in Figs. 6–10. The data for the first four reactions are based on present measurements and those for the  $(n, 2n)$  process on a literature report.<sup>5</sup> In  $^{70}\text{Ge}(\alpha, n)$  reaction the ratio is relatively high at low incident particle energies but decreases with increasing energy (Fig. 6). In the case of  $^{\text{nat}}\text{Ge}(^3\text{He}, xn)$  process up to 24 MeV two reactions, viz.  $^{72}\text{Ge}(^3\text{He}, 2n)$  and  $^{73}\text{Ge}(^3\text{He}, 3n)$ , contribute. Like  $(\alpha, n)$  reaction, the isomeric cross-section ratio is somewhat high at low incident particle energies and decreases with increasing energy (Fig. 7). For  $(p, 3n)$  and  $(d, 4n)$  reactions, on the other hand, the ratio is practically constant over the whole investigated energy range (Figs. 8 and 9). The experimental data on the isomeric cross-section ratio in the  $^{74}\text{Se}(n, 2n)$  process reported in the literature are conflicting. A careful check showed that the results given in Refs. 3 and 4 are erroneous since at the time of those measurements the branching ratio of  $^{73m}\text{Se}$  was not known. We therefore adopted the values

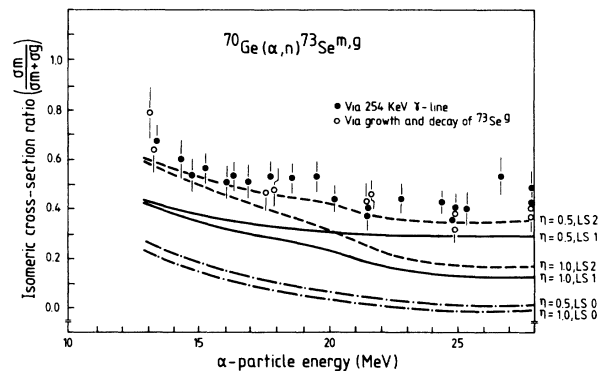


FIG. 6. Isomeric cross-section ratio  $\sigma_m/(\sigma_m+\sigma_g)$  for the isomeric pair  $^{73m,g}\text{Se}$  in  $^{70}\text{Ge}(\alpha, n)$  process. Experimental data (solid and open points) were obtained using two different counting techniques. Results of model calculations using three nuclear level schemes (LS1: 44 discrete levels; LS2: 43 discrete levels; LS0: 2 discrete levels) and two  $\eta$  values (1.0 and 0.5) are shown (for details see text). The best agreement is obtained using LS2 and  $\eta=0.5$ .

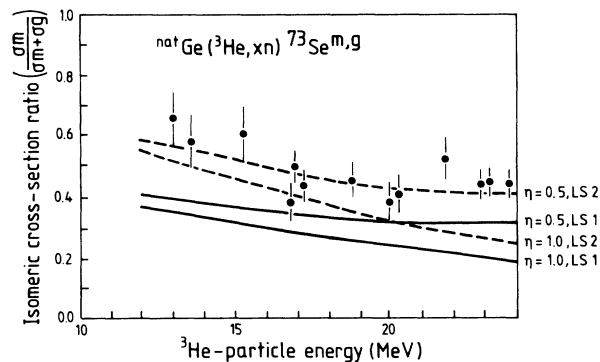


FIG. 7. Isomeric cross-section ratio for the isomeric pair  $^{73m,g}\text{Se}$  in  $^{\text{nat}}\text{Ge}(^3\text{He}, xn)$  process. Experimental data (solid points) and results of model calculations using two nuclear level schemes (LS1 and LS2) and two  $\eta$  values (1.0 and 0.5) are shown.

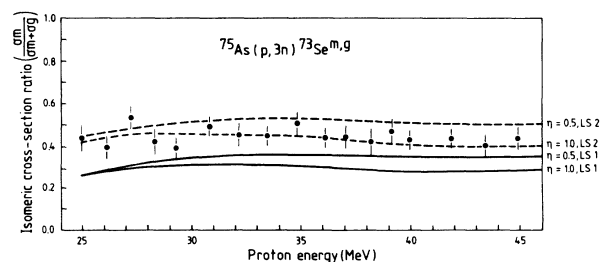


FIG. 8. Isomeric cross-section ratio for the isomeric pair  $^{73m,g}\text{Se}$  in  $^{75}\text{As}(p, 3n)$  reaction. Other details are the same as for Fig. 7.

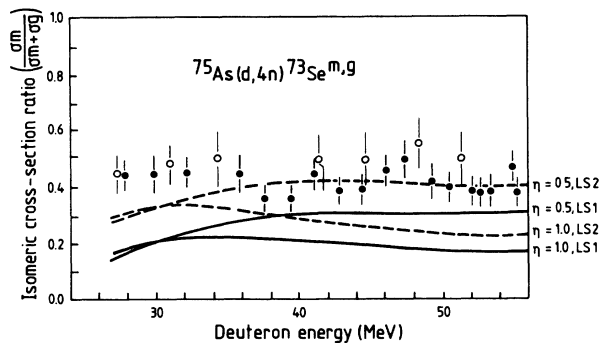


FIG. 9. Isomeric cross-section ratio for the isomeric pair  $^{73m,8}\text{Se}$  in  $^{75}\text{As}(d,4n)^{73}\text{Se}^{m,g}$  reaction. Solid points describe our experimental data and open points those of Ref. 6. Other details are the same as for Fig. 7.

given in Ref. 5. Apart from the early decreasing trend the ratio appears to be constant over the investigated energy range (Fig. 10).

The results of model calculations obtained using the two level schemes (LS1 and LS2) of the product nucleus  $^{73}\text{Se}$  and for  $\eta$  values of 0.5 and 1.0 are given in Figs. 6–10. It appears that the energy dependence of the isomeric cross-section ratio is described best by the assumption  $\Theta_{\text{eff}}/\Theta_{\text{rig}}=0.5$ , and that the absolute values are generally reproduced well by LS2, i.e., by neglecting the level at 26.4 keV. We conclude that either this level does not exist at all or the transitions from the high-lying levels cross over and populate predominantly the isomeric state at 25.7 keV. In general terms the results depict that the isomeric cross-section ratio is strongly dependent on the input level scheme of the product nucleus. If one of the important levels (to which many intermediate transitions occur) is neglected, the calculated isomeric cross-section ratio is drastically changed.

In order to demonstrate the effect of high-spin rotational-band states, calculations were done for the  $^{70}\text{Ge}(\alpha,n)$  process for a hypothetical case, considering only two discrete levels (ground and isomeric states) and

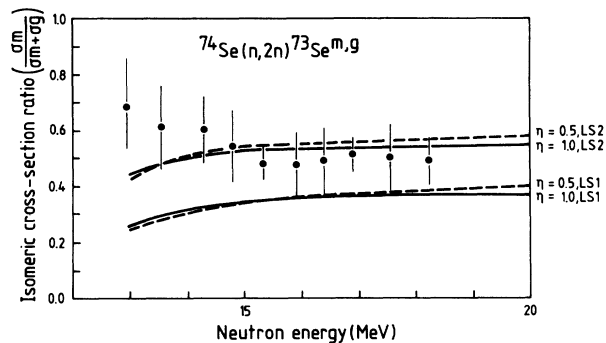


FIG. 10. Isomeric cross-section ratio for the isomeric pair  $^{73m,8}\text{Se}$  in  $^{74}\text{Se}(n,2n)^{73}\text{Se}^{m,g}$  process. Solid points describe the experimental data of Ref. 5. Other details are the same as for Fig. 7.

assuming that the continuum region starts at 100 keV (LS0). As can be seen in Fig. 6 such an assumption leads to a very low isomeric cross-section ratio. Evidently the high-spin discrete levels influence the isomeric cross-section ratio drastically.

Notwithstanding the strong dependence of the isomeric cross-section ratio on the level scheme of the product used, the results given in Figs. 6–10 demonstrate that the compound nucleus model calculations incorporating preequilibrium effects can, under a chosen set of global assumptions, reproduce the isomeric cross-section ratio even in extremely different processes like  $(\alpha,n)$  and  $(p,3n)$ . The method can therefore be possibly used with success for other product nuclei as well.

#### ACKNOWLEDGMENTS

We thank Professor G. Stöcklin for his critical comments on experimental measurements and Professor H. Vonach for some suggestions on model calculations. The Jülich authors thank the crews of the isochronous cyclotron (JULIC) and compact cyclotron (CV 28) for carrying out the irradiations. A. Mushtaq thanks the Deutscher Akademischer Austauschdienst (DAAD) for a stipend.

\*Present address: Pakistan Institute of Nuclear Science and Technology, Islamabad, Pakistan.

<sup>1</sup>Table of Isotopes, 7th ed., edited by C. M. Lederer and V. S. Shirley (Wiley, New York, 1978).

<sup>2</sup>M. M. King, Nucl. Data Sheets **51**, 161 (1987).

<sup>3</sup>M. Bormann, F. Dreyer, U. Seebeck, and W. Voigts, Z. Naturforsch. **21A**, 988 (1966).

<sup>4</sup>A. Abboud, P. Decowski, W. Grochulski, A. Marcinkowski, J. Piotrowski, K. Siwek, and Z. Wilhelmi, Nucl. Phys. **139**, 42 (1969).

<sup>5</sup>M. Bormann, H.-K. Feddersen, H.-H. Hölscher, W. Scobel, and H. Wagener, Z. Phys. A **277**, 203 (1976).

<sup>6</sup>H. F. Röhm, Report No. KFK-1447, 1971 (unpublished).

<sup>7</sup>J. C. Brodovitch, J. J. Hogan, and K. I. Burns, J. Inorg. Nucl. Chem. **38**, 1581 (1976).

<sup>8</sup>M. Guillaume, R. M. Lambrecht, and A. P. Wolf, Int. J. Appl.

Radiat. Isotopes **29**, 411 (1978).

<sup>9</sup>T. Nozaki, Y. Itoh, and K. Ogawa, Int. J. Appl. Radiat. Isotopes **30**, 595 (1979).

<sup>10</sup>R. Weinreich, O. Schult, and G. Stöcklin, Int. J. Appl. Radiat. Isotopes **25**, 535 (1974).

<sup>11</sup>Z. Kovács, G. Blessing, S. M. Qaim, and G. Stöcklin, Int. J. Appl. Radiat. Isotopes **36**, 635 (1985).

<sup>12</sup>F. Tárkányi, S. M. Qaim, and G. Stöcklin, Int. J. Appl. Radiat. Isotopes **39**, 135 (1988).

<sup>13</sup>G. Szekely, J. Electrochem. Soc. **98**, 318 (1951).

<sup>14</sup>S. M. Qaim, G. Blessing, and H. Ollig, Radiochim. Acta **39**, 57 (1986).

<sup>15</sup>A. Mushtaq, S. M. Qaim, and G. Stöcklin, Int. J. Appl. Radiat. Isotopes (in press).

<sup>16</sup>J. Rapaport, V. Kulkani, and R. W. Finlay, Nucl. Phys. **A330**, 15 (1979).

- <sup>17</sup>G. S. Mani, M. A. Melkanoff, and I. Iori, Report CEA-2379, 1963 (unpublished).
- <sup>18</sup>F. Hinterberger, G. Mairle, U. Schmidt-Rohr, G. J. Wagner, and P. Turek, Nucl. Phys. **A111**, 265 (1968).
- <sup>19</sup>F. D. Becchetti, Jr. and G. W. Greenlees, in *Polarization Phenomena in Nuclear Reactions*, edited by H. H. Barschall and W. Haeberli (University of Wisconsin Press, Madison, 1971), p. 682.
- <sup>20</sup>L. McFadden and G. R. Satchler, Nucl. Phys. **84**, 177 (1966).
- <sup>21</sup>D. M. Brink, Ph.D. thesis, Oxford University, 1955; P. Axel, Phys. Rev. **126**, 671 (1962).
- <sup>22</sup>J. M. Blatt and V. F. Weisskopf, *Theoretical Nuclear Physics* (Wiley, New York, 1952), p. 627.
- <sup>23</sup>S. K. Kataria, V. S. Ramamurthy, and S. S. Kapoor, Phys. Rev. C **18**, 549 (1978).
- <sup>24</sup>S. F. Mughabghab, M. Divadeenam, and N. E. Holden, in *Neutron Cross Sections* (Academic, New York, 1981), Vol. I.
- <sup>25</sup>E. Gadioli, E. Erba-Gadioli, and P. G. Sona, Nucl. Phys. **A217**, 589 (1973).
- <sup>26</sup>C. Kalbach, Z. Phys. A **283**, 401 (1977).
- <sup>27</sup>P. Oblozinsky, I. Ribansky, and E. Betak, Nucl. Phys. **A226**, 347 (1974).
- <sup>28</sup>C. Kalbach, Z. Phys. A **287**, 319 (1978).
- <sup>29</sup>H. Feshbach, A. K. Kerman, and S. Koonin, Ann. Phys. (NY) **125**, 429 (1980).
- <sup>30</sup>K. O. Zell, B. Heits, W. Gast, D. Hippe, W. Schuh, and P. von Brentano, Z. Phys. A **279**, 373 (1976).
- <sup>31</sup>M. Uhl, Institut für Radiumforschung und Kernphysik (IRK), University of Vienna (unpublished).
- <sup>32</sup>J. R. Huizenga and G. Igo, Report ANL-6373, 1961 (unpublished).
- <sup>33</sup>M. Blann and J. Bisplinghoff, ALICE/LIVERMORE82, Report UCID-19614, 1982 (unpublished).